

## Characterization of Fe states in dilute $^{57}\text{Mn}$ implanted $\text{SnO}_2$ film

H. P. Gunnlaugsson · K. Nomura · T. E. Mølholt ·  
S. Shayestehaminzadeh · K. Johnston · R. Mantovan ·  
H. Masenda · M. Ncube · K. Bharuth-Ram · H. Gislason ·  
G. Langouche · D. Naidoo · S. Ólafsson ·  
G. Weyer · the ISOLDE Collaboration

© Springer Science+Business Media Dordrecht 2013

**Abstract** States of dilute Fe in  $\text{SnO}_2$  have been monitored using  $^{57}\text{Fe}$  emission Mössbauer spectroscopy following implantation of  $^{57}\text{Mn}$  ( $T_{1/2} = 85.4$  s) in the temperature range from 143 K to 711 K. A sharp annealing stage is observed at  $\sim 330$  K where the  $\text{Fe}^{3+}/\text{Fe}^{2+}$  ratio shows a marked increase. It is suggested that this annealing stage is due to the dissociation of Mn-V<sub>O</sub> pairs during the lifetime of  $^{57}\text{Mn}$ ; the activation energy for this dissociation is estimated to be 0.9(1) eV.  $\text{Fe}^{3+}$  is found in a paramagnetic state showing spin-lattice relaxation rates consistent with

---

Proceedings of the 32nd International Conference on the Applications of the Mössbauer Effect (ICAME 2013) held in Opatija, Croatia, 1–6 September 2013.

H. P. Gunnlaugsson (✉) · G. Weyer  
Department of Physics and Astronomy, Aarhus University, 8000 Aarhus, Denmark  
e-mail: hpg@phys.au.dk

K. Nomura  
School of Engineering, The University of Tokyo, Tokyo 113-8656, Japan

T. E. Mølholt · S. Shayestehaminzadeh · H. Gislason · S. Ólafsson  
Science Institute, University of Iceland, 107 Reykjavík, Iceland

K. Johnston · the ISOLDE Collaboration  
PH Department, ISOLDE/CERN, 1211 Geneva 23, Switzerland

R. Mantovan  
Laboratorio MDM, IMM-CNR, Via Olivetti 2, 20864 Agrate Brianza MB, Italy

H. Masenda · M. Ncube · D. Naidoo  
School of Physics, University of the Witwatersrand, Johannesburg, South Africa

K. Bharuth-Ram  
School of Physics, Durban University of Technology, Durban 4000, South Africa

G. Langouche  
Instituut voor Kern-en Stralings fysika, University of Leuven, 3001 Leuven, Belgium

an expected  $T^2$  dependence derived for a Raman process. In addition, a sharp lined doublet in the Mössbauer spectra is interpreted as due to recoil produced interstitial Fe.

**Keywords**  $\text{SnO}_2$  ·  $^{57}\text{Mn}$  implantation · Emission Mössbauer spectroscopy · Defects

## 1 Introduction

Following the theoretical prediction made by Dietl et al. about room temperature ferromagnetism in dilute 3d metal doped ZnO [1] there has been increasing interest in investigating the structural, chemical, and magnetic properties of 3d-doped semiconductors and oxides, due to their potential applications in spintronic devices.

Tin dioxide with rutile structure has been suggested as a potential dilute ferromagnetic material if doped with Fe [2]. “Volume-sensitive” magnetic measurements have led to the suggestion that the magnetic ordering could originate from the coupling of 3d metals to structural defects [2, 3].

Following the proposal of the existence of a charge-transfer based dilute ferromagnetic ordering by Coey and co-workers [4, 5], it has become of particular importance to identify charge state(s) of Fe in Fe-doped  $\text{SnO}_2$ . Techniques sensitive at the atomic scale are required to evaluate potential correlations between the observed magnetic properties and the charge state of Fe dopants.

Bhide and Date [6] investigated  $^{57}\text{Fe}$  Mössbauer spectra of  $\text{SnO}_2$  samples doped with  $^{57}\text{Fe}$  in the range from 0.2 to 2 at.%. At the lowest concentration, they observed  $\text{Fe}^{3+}$  showing slow paramagnetic relaxation, and an increased relaxation rate at higher concentrations due to spin-spin relaxations. Mössbauer spectroscopy of  $\text{SnO}_2$  samples implanted with stable  $^{57}\text{Fe}$  at  $\sim 5$  at.% [7], show that precipitation takes place upon high temperature implantation or post-annealing.

Here we present the results of emission Mössbauer spectroscopy measurements on  $\text{SnO}_2$  doped with extremely dilute concentrations of Fe ( $\sim 5 \times 10^{-4}$  at.%) following implantation of  $^{57}\text{Mn}$  ( $T_{1/2} = 1.5$  min). The polycrystalline  $\text{SnO}_2$  thin films studied here were made by DC sputtering of  $\text{SnO}_2$  target on quartz. The samples (around 250 nm thick) were annealed at 550 °C for 2 h in air atmosphere which should remove most of any possible non-stoichiometry (presence of SnO). Samples made in the same way have been investigated with higher doses  $^{57}\text{Fe}$  and  $^{119}\text{Sn}$  implantations [8].

## 2 Experimental

Pure beams of  $^{57}\text{Mn}^+$  ( $T_{1/2} = 85.4$  s) were produced at the ISOLDE facility at CERN following 1.4 GeV proton induced fission in a heated  $\text{UC}_2$  target and elemental selective laser ionization [9] with a current of a few times  $10^8$   $^{57}\text{Mn}/\text{s}$ . After acceleration to 40 keV, the beam was implanted at incident angle of  $\theta_1 = 30^\circ$  relative to the sample normal into samples of  $\text{SnO}_2$ .

$^{57}\text{Fe}$  emission Mössbauer spectra were recorded at emission angle  $\theta_E = 60^\circ$  relative to the sample normal using a single-line resonance detector equipped with  $^{57}\text{Fe}$  enriched stainless-steel electrodes, mounted on a conventional drive system

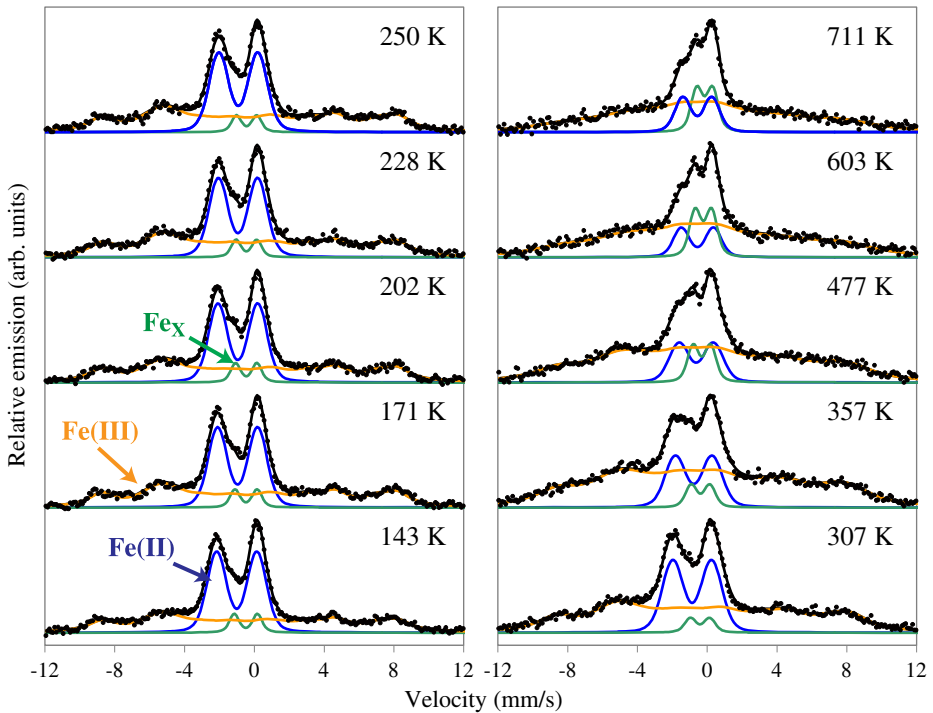


**Fig. 1**  $^{57}\text{Fe}$  emission Mössbauer spectra obtained after implantation of  $^{57}\text{Mn}$  into  $\text{SnO}_2$  samples held at the temperatures indicated. The solid lines indicate the fitting components (as marked) and their sum

outside the implantation chamber. In all cases, samples were implanted with a total fluence  $< 2 \times 10^{12}$   $^{57}\text{Mn}/\text{cm}^2$ , corresponding to a maximum local concentration of  $\sim 5 \times 10^{-4}$  at.%. Isomer shifts and velocities are given relative to the centre of the spectrum of  $\alpha\text{-Fe}$  at room temperature (RT).

In the  $\beta^-$  decay of  $^{57}\text{Mn}$  the daughter  $^{57}\text{Fe}$  atom is given an average recoil energy of  $\langle E_R \rangle = 40$  eV (maximum  $E_{R,\text{max}} = 93$  eV), leading to the possible formation of interstitial Fe in the case the bond-dissociation energy is less than the recoil energy.

### 3 Results and analysis

The spectra obtained (cf. Fig 1) have been analysed in terms of three components: (1) a doublet marked Fe(II), assigned to high-spin  $\text{Fe}^{2+}$  simulated as a symmetric doublet with a Gaussian distribution of quadrupole splittings; (2) a magnetic hyperfine field distribution marked Fe(III), assigned to high-spin  $\text{Fe}^{3+}$  showing slow (temperature dependent) paramagnetic relaxations analysed in terms of an empirical model (EmpBT) [10, 11]; (3) a doublet component,  $\text{Fe}_X$ , tentatively assigned to interstitial Fe.

The spectra measured in the high temperature setup ( $T \geq 307$  K) turned out to have slightly broader lines than the spectra obtained in the low temperature setup

**Fig. 2** Relative spectral areas extracted from the analysis of the spectra in Fig. 1

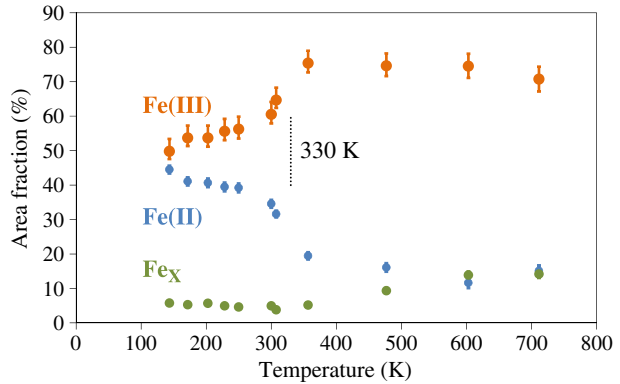
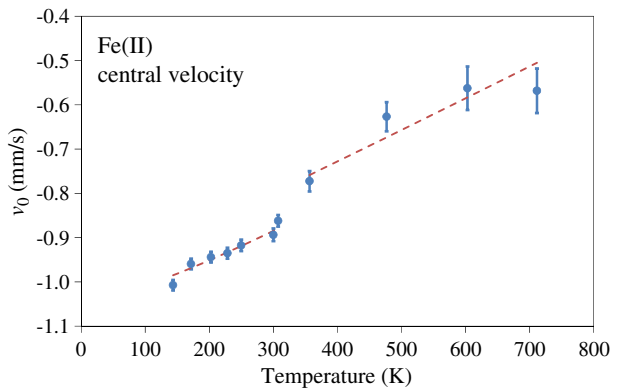


**Fig. 3** Central velocity ( $v_0$ ) of the Fe(II) component as a function of temperature. The dashed lines show the tendency expected from a SOD behaviour in the high and low temperature regions



( $T \leq 300$  K). This was identified to be caused by additional vibrations in the high temperature setup, which has been accounted for in the simultaneous analysis.

The doublet marked  $\text{Fe}_X$  is only clearly visible in the spectra above 477 K, and its presence at lower temperatures can be inferred from the asymmetrical broadening of the central part of the more dominant Fe(II) component. Due to the small relative intensity of the  $\text{Fe}_X$  component it was analysed with a temperature independent line-width and the central position was set to follow the second order Doppler (SOD) shift with temperature. Above 350 K, the splitting shows a slight reduction, and in the final analysis, the quadrupole splitting of the  $\text{Fe}_X$  component was assumed to follow a power law,  $\Delta E_Q(T) = a \cdot T^{-b}$ , where  $a$  and  $b$  are fitting variables. This restriction is not unique and different types of temperature dependence are possible. In all cases, the quadrupole splitting at room temperature is  $\Delta E_Q = 1.1(1)$  mm/s, reducing to  $\Delta E_Q = 0.9(1)$  mm/s at 711 K. The isomer shift of  $\text{Fe}_X$  is determined to be  $\delta = 0.42(2)$  mm/s. The line-width ( $\Gamma = 0.34$  mm/s and  $\sigma = 0.095(10)$  mm/s) is practically identical to the detector line-width, suggesting negligible broadening in excess of the natural line-width.

The relative spectral areas, displayed in Fig. 2, demonstrate an annealing stage at  $\sim 330$  K, where a fraction of the Fe(II) is transformed into Fe(III).

The central velocity of the Fe(II) component as a function of temperature (cf. Fig. 3) does not follow the SOD throughout the temperature range. There is a

**Fig. 4** Quadrupole splitting of Fe(II) as a function of temperature. The *dashed line* shows a tendency expected for a temperature dependent population of the 3d orbitals

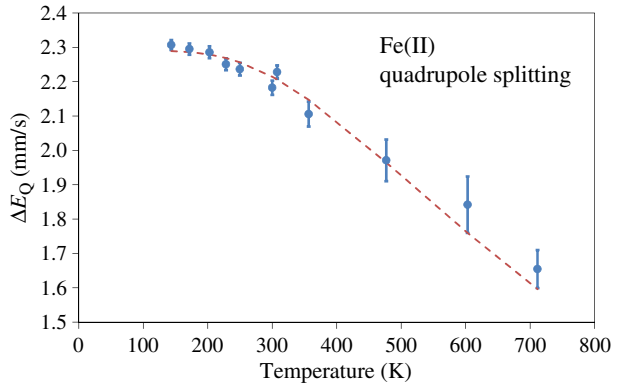
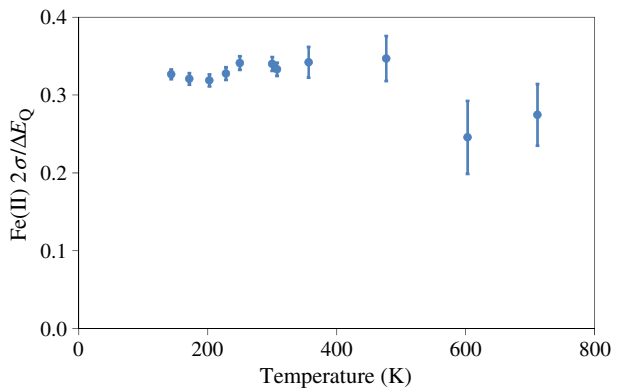


**Fig. 5** Relative Gaussian line-width of the quadrupole splitting distribution of the Fe(II) component as a function of temperature

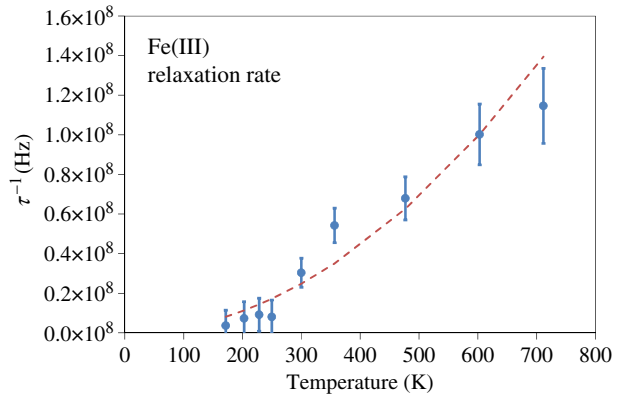


kink in the curve at temperatures between 307 K and 357 K, matching the annealing stage as seen in the relative areas of the spectral components (cf. Fig. 2). The data at  $T \leq 307$  K yields an isomer shift of  $\delta = 0.885(5)$  mm/s at RT, while the data at  $T \geq 356$  K suggests a lower value of  $\delta = 0.79(2)$  mm/s extrapolated to RT. These isomer shift values are lower than those determined from higher dose <sup>57</sup>Fe implantations into the same type of samples [8], suggesting a fluence dependence of the isomer shift.

On the other hand, there is no sharp change in the quadrupole splitting around 330 K (cf. Fig. 4), indicating that the annealing stage seen in the relative area and isomer shift do not affect the quadrupole interaction of Fe<sup>2+</sup> significantly. A decrease of the quadrupole interaction through the temperature range is observed as expected for a temperature dependent population of the 3d orbitals. The RT quadrupole splitting ( $\Delta E_Q = 2.20(5)$  mm/s) is significantly higher than that found for Fe<sup>2+</sup> at higher fluence <sup>57</sup>Fe implantations [7, 8].

The relative Gaussian line-width of the quadrupole splitting distribution ( $2\sigma/\Delta E_Q$ ) of the Fe(II) component (cf. Fig. 5) is roughly constant at  $T < 500$  K, and indicates a small decrease at higher temperatures. The same ratio for Fe<sup>2+</sup> in amorphous environments observed in  $\alpha$ -Al<sub>2</sub>O<sub>3</sub> [12] and MgO [11] (see discussion in [13]) have values between 0.3 and 0.4 at low temperatures, but increases to 0.5–0.6 at elevated temperatures (600–700 K) as the quadrupole splitting decreases.

**Fig. 6** Temperature dependence of the spin relaxation rate of Fe(III) compared to a  $T^2$  dependence (dashed line)



This is clearly not the case here. This temperature dependence is consistent with  $\text{Fe}^{2+}$  in amorphous regions at low temperatures, while the  $\text{Fe}^{2+}$  at higher temperatures likely must be in a more regular environment, most probably associated with charge compensating defect(s).

The temperature dependence of the spin relaxation rate, as determined within the EmpBT model from the line broadening of the sextet features in the spectra, is displayed in Fig. 6. Generally, the observed line broadening,  $\Gamma_{\text{Obs}}$ , can be written:

$$\Gamma_{\text{Obs}} = \Gamma_{\text{Det}} + \Gamma_{\text{Env}} + \frac{2\hbar c\tau^{-1}}{E_0}$$

where  $\Gamma_{\text{Det}}$  is the experimental line-width taking into account geometrical broadening and the detector resolution ( $\sim 1$  mm/s for the outermost lines),  $\Gamma_{\text{Env}}$  is the broadening due to inhomogeneous local surroundings, and  $\tau^{-1}$  is the relaxation rate. In the EmpBT model it is assumed that the relaxation rate is negligible at the lowest temperature ( $\tau^{-1} = 0$ ) and the intrinsic values of  $\Gamma_{\text{Det}} + \Gamma_{\text{Env}}$  is temperature independent.

The annealing stage at  $\sim 330$  K is an obvious problem. If the  $\text{SnO}_2$  material becomes more “crystalline” at this temperature it is likely that  $\Gamma_{\text{Env}}$  is not constant through the temperature series and a “sharpening” could be expected at  $\sim 330$  K. This is not obvious in Fig. 6, where the relaxation rate follows an assumed  $T^2$  dependence. We can conclude that the data are not inconsistent with a  $T^2$  dependence. With  $\tau^{-1} = AT^2$ , one obtains  $A = 275(23) \text{ s}^{-1} \text{ K}^{-2}$  and an intrinsic line-width  $\Gamma_{\text{Det}} + \Gamma_{\text{Env}} = 1.7$  mm/s.

## 4 Discussion

There is a clear sharp annealing stage at  $\sim 330$  K, where a fraction of the Fe(II) is transformed into Fe(III). A similar annealing stage after  $^{57}\text{Mn}/^{57}\text{Fe}$  implantation into  $\text{TiO}_2$  rutile was observed at  $\sim 550$  K [13] and suggested to be due to dissociation of Mn- $\text{V}_\text{O}$  pairs during the lifetime of  $^{57}\text{Mn}$ . In a single step annealing model, where effects of re-trapping are neglected, the activation energy of dissociation can be estimated as  $E_a = kT_A \ln(\nu_0\tau)$  where  $k$  is the Boltzmann constant,  $T_A$  the annealing

temperature,  $\nu_0$  the attempt frequency which should be of the order of the lattice vibrations ( $10^{11}$ – $10^{13}$  Hz), and  $\tau$  is the lifetime of  $^{57}\text{Mn}$  (85.4 s). This gives an estimate of the activation energy of dissociation of Mn-V<sub>O</sub> pairs in SnO<sub>2</sub> of  $E_a = 0.9(1)$  eV.

In light of the recoil imparted on the Fe atom in the  $\beta^-$  decay of  $^{57}\text{Mn}$ , it is tempting to assign Fe<sub>X</sub> to interstitial Fe. This interpretation is consistent with the fact that this component is observed with a negligible broadening. While the hyperfine parameters of substitutional Fe defects are very sensitive to lattice imperfections due to the strong bonding to lattice atoms, the same is not expected for interstitial defects. Fe<sub>X</sub> has a rather similar isomer shift as components assigned to interstitial Fe in other oxides (0.55(2) mm/s in ZnO [14] and 0.54(1) mm/s in  $\alpha$ -Al<sub>2</sub>O<sub>3</sub> [12]) and has not been observed in SnO<sub>2</sub> samples implanted with stable  $^{57}\text{Fe}$  [6–8] where the same magnitude of recoil is not present. Below 300 K a constant area fraction of  $\sim 5\%$  is observed as would be expected for recoil-produced interstitial defects, although above RT, the relative Fe<sub>X</sub> area increases to  $\sim 14\%$  at  $\sim 700$  K. This observation is not consistent with the interpretation as recoil produced interstitial defects and additionally, interstitial defects are expected to have lower Debye temperatures than substitutional defects, resulting in less relative area at higher temperatures. On the other hand, the interpretation of the Fe<sub>X</sub> component as due to interstitial Fe, can be supported by assuming a temperature dependent displacement energy. Such temperature dependence has been reported in  $\alpha$ -Al<sub>2</sub>O<sub>3</sub> [15] and MgO [16], but to our knowledge, data on SnO<sub>2</sub> are not available. Another possible explanation is that Fe atoms that are relocated from a substitutional site due to the recoil in the  $\beta^-$  decay in an environment characterized by a high concentration of vacancy defects can more easily be incorporated into substitutional sites. Consequently, as the defects density reduces at elevated temperatures, the probability for observing interstitial Fe increases.

## 5 Conclusions

$^{57}\text{Fe}$  emission Mössbauer spectroscopy following implantation of  $^{57}\text{Mn}$  ( $T_{1/2} = 85.4$  s) to a maximum local concentration of  $5 \times 10^{-4}$  at.% into SnO<sub>2</sub> samples show a sharp annealing stage at  $\sim 330$  K where the Fe<sup>3+</sup> fraction increases. It is suggested that this annealing stage is due to dissociation of Mn-V<sub>O</sub> pairs; the activation energy for dissociation is estimated to be 0.9(1) eV. No evidence of ferromagnetism is observed, instead Fe<sup>3+</sup> is found in paramagnetic state showing spin-lattice relaxation rates consistent with an expected  $T^2$  dependence derived for a Raman process. A sharp lined doublet is interpreted as due to recoil produced interstitial Fe.

**Acknowledgements** This work was supported by the European Union Seventh Framework through ENSAR (contract no. 262010). R. Mantovan acknowledges support from MIUR through the FIRB Project RBAP115AYN “Oxides at the nanoscale: multifunctionality and applications”. K. Bharuth-Ram, H. Masenda, D. Naidoo and M. Ncube acknowledge support from the South African National Research Foundation and the Department of Science and Technology. T. E. Møhlholt, H. Gislason, and S. Olafsson acknowledge support from the Icelandic Research Fund. Financial support of the German BMBF Contract No. 05KK4TS1/9 is also gratefully acknowledged.

## References

1. Dietl, T., Ohno, H., Matsukura, F., Cibert, J., Ferrand, D.: Zener model description of ferromagnetism in zinc-blende magnetic semiconductors. *Science* **287**, 1019–1022 (2000)
2. Coey, J.M.D., Douvalis, A.P., Fitzgerald, C.B., Venkatesan, M.: Ferromagnetism in Fe-doped SnO<sub>2</sub> thin films. *Appl. Phys. Lett.* **84**, 1332–1334 (2004)
3. Fitzgerald, C.B., Venkatesan, M., Dorneles, L.S., Gunning, R., Stamenov, P., Coey, J.M.D., Stampe, P.A., Kennedy, R.J., Moreira, E.C., Sias, U.S.: Magnetism in dilute magnetic oxide thin films based on SnO<sub>2</sub>. *Phys. Rev.* **B74**, 115307 (2006)
4. Coey, J.M.D., Wongsaprom, K., Alaria, J., Venkatesan, M.: Charge-transfer ferromagnetism in oxide nanoparticles. *J. Phys. D. Appl. Phys.* **41**, 134012 (2008)
5. Coey, J.M.D., Stamenov, P., Gunning, R.D., Venkatesan, M., Paul, K.: Ferromagnetism in defect-ridden oxides and related materials. *New J. Phys.* **12**, 053025 (2010)
6. Bhide, V.G., Date, S.K.: Mössbauer effect for <sup>57</sup>Fe in SnO<sub>2</sub>. *J. Inorg. Nucl. Chem.* **31**, 2397–2407 (1969)
7. Nomura, K., Iio, S., Hirose, Y., Reuther, H., Nakanishi, A.: Magnetic behaviour and DCMS study of SnO<sub>2</sub> films implanted with <sup>57</sup>Fe. *Hyperfine Interact.* **217**, 37–43 (2013)
8. Nomura, K., Reuther, H.: Nano-structure analysis of Fe implanted SnO<sub>2</sub> films by <sup>57</sup>Fe and <sup>119</sup>Sr DCMS. *Hyperfine Interact.* **191**, 159–165 (2009)
9. Fedoseyev, V.N., Bätzner, K., Catherall, R., Evens, A.H.M., Forkel-Wirth, D., Jonsson, O.C., Kugler, E., Lettry, J., Mishin, V.I., Ravn, H.L., Weyer, G., the ISOLDE Collaboration: Chemically selective laser ion source of manganese. *Nucl. Inst. Methods B* **126**, 88–91 (1997)
10. Møhlholt, T.E., Mantovan, R., Gunnlaugsson, H.P., Naidoo, D., Ólafsson, S., Bharuth-Ram, K., Fanciulli, M., Johnston, K., Kobayashi, Y., Langouche, G., Masenda, H., Sielemann, R., Weyer G., Gíslason, H.P.: Observation of spin-lattice relaxations of dilute Fe<sup>3+</sup> in MgO by Mössbauer spectroscopy. *Hyperfine Interact.* **197**, 89–94 (2010)
11. Møhlholt, T.E., Gunnlaugsson, H.P., Johnston, K., Mantovan, R., Masenda, H., Ólafsson, S., Bharuth-Ram, K., Gíslason, H.P., Langouche, G., Weyer G., the ISOLDE Collaboration: Spin-lattice relaxations of paramagnetic Fe<sup>3+</sup> in ZnO. *Phys. Scr.* **T148**, 014006 (2012)
12. Gunnlaugsson, H.P., Mantovan, R., Møhlholt, T.E., Naidoo, D., Johnston, K., Masenda, H., Bharuth-Ram, K., Langouche, G., Ólafsson, S., Sielemann, R., Weyer, G., Kobayashi, Y., the ISOLDE Collaboration: Mössbauer spectroscopy of <sup>57</sup>Fe in  $\alpha$ -Al<sub>2</sub>O<sub>3</sub> following implantation of <sup>57</sup>Mn\*. *Hyperfine Interact.* **198**, 5–13 (2010)
13. Gunnlaugsson, H.P., Mantovan, R., Masenda, H., Møhlholt, T.E., Johnston, K., Bharuth-Ram, K., Gíslason, H., Langouche, G., Naidoo, D., Ólafsson, S., Svane, A., Weyer, G., the ISOLDE collaboration: Manuscript in preparation (2013)
14. Weyer, G., Gunnlaugsson, H.P., Mantovan, R., Naidoo, D., Bharuth-Ram, K., Fanciulli, M., Agne, T.: Defect-related local magnetism at dilute Fe atoms in ion-implanted ZnO. *J. Appl. Phys.* **102**, 113915 (2007)
15. Pells, G.P., Phillips, D.C.: Radiation damage of  $\alpha$ -Al<sub>2</sub>O<sub>3</sub> in the HVEM. *J. Nucl. Mater.* **80**, 207–214 (1979)
16. Pells, G.P.: The temperature dependence of the threshold displacement energy in MgO. *Radiat. Eff.* **64**, 71–75 (1982)